fermentation

MDPI

Article

Olive Pruning: Waste or Growth Media? Expanding the Metabolic Potential of Phyllospheric *Rhodococcus* sp. 24CO

Natalia E. Sandoval [1], Margarita Gomila [2], Nadia S. Arias [1], Héctor M. Alvarez [1] and Mariana P. Lanfranconi [1,*]

[1] INBIOP (Instituto de Biociencias de la Patagonia), Consejo Nacional de Investigaciones Científicas y Técnicas, Facultad de Ciencias Naturales y Ciencias de la Salud, Universidad Nacional de la Patagonia San Juan Bosco, Ruta Provincial N° 1, Km 4-Ciudad Universitaria, Comodoro Rivadavia 9000, Argentina; nsandoval@cenpat-conicet.gob.ar (N.E.S.); narias@cenpat-conicet.gob.ar (N.S.A.); halvarez@unpata.edu.ar (H.M.A.)

[2] Microbiologia, Departament Biologia, Universitat de les Illes Balears, 07122 Palma, Spain; marga.gomila@uib.es

* Correspondence: mlanfranconi@unpata.edu.ar

Abstract: *Rhodococcus* sp. 24CO, isolated from the olive phyllosphere, can accumulate significant amounts of neutral lipids, making it a promising candidate for biomass production from olive pruning waste. The strain efficiently converts this residue to neutral lipids, achieving a yield of over 20% of the cellular dry weight (CDW). This indicates that olive leaves, a by-product of the olive oil industry, could become a valuable resource for both the economy and the environment. Genome analysis revealed various metabolic pathways for converting carbon sources to neutral lipids, while phenotypic studies showed that the strain is selective about its carbon sources, thriving on specific monosaccharides and polyols found in olive leaves. Notably, fructose and mannitol were rapidly metabolized, leading to a content of stored triacylglycerides of up to 47% and 28% of the CDW, respectively. The strain also exhibited oleagenicity under high nitrogen availability when grown on mannitol. Finally, potential oleagenicity determinants were explored through an omics comparison.

Keywords: olive pruning waste; neutral lipid storage; *Rhodococcus*; oleagenicity; polyols

check for updates

Academic Editor: Alessia Tropea

Received: 1 March 2025
Revised: 15 April 2025
Accepted: 16 April 2025
Published: 23 April 2025

Citation: Sandoval, N.E.; Gomila, M.; Arias, N.S.; Alvarez, H.M.; Lanfranconi, M.P. Olive Pruning: Waste or Growth Media? Expanding the Metabolic Potential of Phyllospheric *Rhodococcus* sp. 24CO. *Fermentation* **2025**, *11*, 237. https://doi.org/10.3390/fermentation11050237

Copyright: © 2025 by the authors. Licensee MDPI, Basel, Switzerland. This article is an open access article distributed under the terms and conditions of the Creative Commons Attribution (CC BY) license (https://creativecommons.org/licenses/by/4.0/).

1. Introduction

Members of the *Rhodococcus* genus are aerobic, Gram-positive, and non-motile with a high GC content and mycolic acids containing cell walls [1]. Representatives of this genus are typically found in marine sediments, soil and water and there are two pathogenic species, *R. fascians* and *R. hoagii*, affecting plants and animals, respectively [2]. Representatives affiliated with *Rhodococcus* have also been recovered from stressful environments such as polluted Antarctic and Patagonian soils [3,4]. Particularly, bacterial isolates in Patagonia must cope with desiccation, high UV radiation and nutrient limitation, conditions that are present in the surface of leaves [5].

Leaves are the primary photosynthetic organ in plants with an adaxial or upper surface and an abaxial or lower surface [6]. The phyllosphere is a vast area of the plant that surrounds its leaves, also being a niche for diverse groups of microorganisms. In contrast to the largely studied rhizosphere, phyllosphere bacteria have often been ignored [7]. Microorganisms associated with the leaf surface go beyond pathogens and although it is a harsh environment, bacteria survive in the phyllosphere and could have positive, negative or neutral interactions with the plant [8,9]. Rhodococcal bacterial strains from phyllosphere have been isolated on the leaf surfaces of different plants [10,11]. However,

their metabolic potential is scarcely reported and their biotechnological potential is mostly limited to xenobiotics biodegradation [12,13].

The ability of *Rhodococcus* to thrive in extreme habitats depends on their metabolic characteristics, which usually contribute to their biotechnological applications [14]. In this context, the capability for the biodegradation of hydrocarbons and other xenobiotics is a remarkable characteristic of this genus [15]. Taking advantage of omics techniques, degradation pathways present in *Rhodococcus* strains have been revealed [16,17]. These strains are also considered ideal biofactories due to their innate ability to produce diverse compounds such as biosurfactants, triacylglycerides, polyhydroxyalkanoates and carotenoids in significant amounts [18]. Triacylglycerides (TAG) accumulation in *Rhodococcus* is known to be adaptation to harsh environmental conditions [18,19], and triacylglycerides are a biotechnological product with application in different industries [14]. Some species belonging to the *Rhodococcus* genus are considered as oleaginous, as they produce more than 20% *w*/*w* of their cellular dry weight (CDW) when grown under different carbon sources and under controlled conditions [14]. Waste such as whey, molasses and olive and fruit juices derived from diverse agro-industries has also been efficiently converted into TAGs with high biomass and TAG yields [14,20]. Diverse carbon sources have been evaluated to find those that can be more efficiently transformed into TAGs. However, natural polyols, such as mannitol, have never been studied. Mannitol is the most abundant polyol found in fungi, plants and algae [21]. It accumulates at high concentrations in the aerial organs of some plants, being particularly abundant in olive leaves [22,23] but also having been found and studied in celery [24]. It is a major photosynthetic product that is not completely translocated to other organs and acts as an osmoprotectant when drought affects the plant [24].

Olive trees are widely distributed around the world, especially in the Mediterranean Basin. In recent decades, different cultivars have been established at higher latitudes, like in the coastal area of Patagonia [25]. This region is characterized by its cold and semi-dry climate. The olive industry in Argentina is relevant, although smaller than to the olive industry in the European region, which represents 90% of world olive production [26]. It generates different by-products, such as olive mill wastewater [27] and solid waste such as alperujo and orujo [28] and the valorization of these residues have been largely reported [29]. In Spain in particular, the olive industry generates 1.25 million tons of leaves per year from pruning [30]. The recycling of olive pruning waste could protect the environment and improve the use of a natural resource, however, it is usually burned. This agriculture by-product represents an untapped, mannitol-rich biomass that could be redirected toward sustainable bioprocessing resulting in the production of TAGs as value added compounds. To achieve this goal, we report the isolation of a novel bacterial strain, *Rhodococcus* sp. 24CO, from the phyllosphere of an olive tree cultivated in Patagonia. We characterized its growth and metabolic traits, with a particular focus on its capacity to synthesize TAGs from olive pruning waste. To evaluate the potential of in *Rhodococcus* sp. 24CO in TAG production, we merged analysis of its genome with the characterization of TAG synthesis under different carbon sources, including those usually found in olive leaves.

2. Materials and Methods

2.1. Isolation of Strain 24CO

The strain was isolated from the phyllosphere of *Olea europaea* var. frantoio growing on the Patagonian coast (45°47′53″ S; 67°24′59″ W). During autumn, healthy olive leaves were aseptically cut from trees and placed in a sterile bag. After arrival at the laboratory, the collected leaves were washed twice with a sterile 0.85% NaCl *w*/*v* solution and imprinted (abaxial or adaxial side) on nutrient broth agar plates with cycloheximide (10 µg/mL) to

avoid fungal growth. The plates were kept at 28 °C for 4 days. Once isolated, the strain was grown aerobically at 28 °C in Luria-Bertani (LB) agar broth and conserved at 4 °C.

2.2. Morphology and Growth Characteristics

The cell morphology was examined by light microscopy using Gram staining. The growth at different temperatures (4 °C, 8 °C, 28 °C, 30 °C and 37 °C), pH values (from 5 to 12) and NaCl concentrations (from 1 to 7% w/v) was tested in an LB medium using liquid LB broth as the inoculum. For each condition except the temperature, the growth was recorded after 3 days of incubation at 28 °C with agitation at 200 rpm. The growth with different carbon sources was tested in triplicates using a minimal salt medium (MSM). The MSM (1 L) was prepared with 1.5 g KH_2PO_4; 9 g $Na_2HPO_4{\cdot}12H_2O$; 0.2 g $MgSO_4{\cdot}7H_2O$; 1.2 mg FeNH4-Citrate; 20 mg $CaCl_2{\cdot}2H_2O$ and 0.1 mL SL6 solution (10 mg $ZnSO_2{\cdot}7H_2O$; 3 mg $MnCl_2{\cdot}4H_2O$; 30 mg H_3BO_3; 20 mg $CoCl_2{\cdot}6H_2O$; 1 mg $CuCl_2{\cdot}2H_2O$; 2 mg $NiCl_2{\cdot}6H_2O$; 3 mg $Na_2MoO_4{\cdot}2H_2O$ per L). In addition, NH_4Cl was added at a concentration of 1 or 0.1 g L/L to prepare MSM1 or MSM0.1, respectively [31]. The former, with no nitrogen-limiting condition (1 g/L) was used to assess growth and the latter, to induce nitrogen starvation due to a low content of nitrogen (0.1 g/L), allowing for neutral lipid accumulation (storage conditions). Carbon sources were added at a final concentration of 1% (w/v), except for glycerol, which was used at a concentration of 0.3% (v/v). The growth was recorded by measuring the optical density at a wavelength of 600 nanometers (OD600). To cultivate cells in both MSM, a liquid LB preculture was inoculated after a colony was picked from a fresh plate and grown overnight. After growing for 10 h, the cells were collected, washed twice with sterile saline solution and used to inoculate the media (initial OD600 of 0.2). Furthermore, a deeper study of the utilization of carbon sources was conducted on an API 50CH (Biomerieux, Marcy-l'Étoile, France), following the manufacturer instructions. The results of assimilation and fermentation were recorded at 24, 48 and 96 h.

2.3. Genome Sequencing, Assembly and Annotation

Genomic DNA was extracted using the FastDNA spin kit for soil (MP Biomedicals, Solon, OH, USA). The quality of the obtained DNA was analyzed by agarose gel electrophoresis and then quantified in a Qubit 3.0 Fluorometer (Life Technologies, Carlsbad, CA, USA). Genomic DNA was sequenced with an Illumina NovaSeq6000 platform produced by Macrogen Inc., Seoul, Republic of Korea after library construction. Raw sequence reads were quality filtered using a Trimmomatic v0.39 [32] and deduplicated using Clumpify from BBTools v38.18 [33]. De novo assembly was performed with Spades (v3.15.3) using the KBase platform [34]. Genome annotation was performed using (i) the Subsystem Technology platform v2.0 (RAST) with default parameters [35], (ii) the Bacterial and Viral Bioinformatics Resource Center (BV-BRC) v3.32.13a [36] and (iii) the NCBI Prokaryotic Genome Annotation Pipeline (PGAP). The identification of contigs containing plasmid-like sequences from the draft genome was performed using PLASMe v1.1 [37].

2.4. Phylogenetic Analysis

Phylogenetic analysis was performed using the Type Strain Genome server (TYGS) and a whole genome phylogenetic tree based on core genes [38] with the most closely related strains created to assess their phylogenetic affiliation.

2.5. Reconstruction of Catabolic Pathways

The reconstruction of catabolic pathways in *Rhodococcus* sp. 24CO was based on RAST annotation, followed by the submission of the annotations to the KASS server [39]. To ensure the accuracy of our findings, genes related to the Kennedy pathway and transporters associated with optimal carbon sources underwent a thorough BLAST search (v. 2.15.0) in

the NCBI database. For homologous gene identification, a minimum coverage of 80% and an identity of at least 60% were used when the reference protein originated from *Rhodococcus* species [40]. In cases where the BLAST compared proteins at the phylum level (with those of *Mycobacterium* or *Streptomyces*), homologous gene identities exceeding 40% and a coverage of 70% were considered relevant [20]. Additionally, we investigated the occurrence of the shared synteny of catabolic clusters between 24CO and other *Rhodococcus* species, which was indicative of shared functionality. Furthermore, to confirm the annotation, we cross-referenced hits with the NCBI Conserved Domain (CD), adding another layer of confidence to our functional predictions.

2.6. Neutral Lipid Accumulation from Selected Carbon Sources

Qualitative analyses of the total intracellular lipids were performed using samples collected at the beginning of the stationary phase by thin layer chromatography (TLC). For this, 5 mg of dried cells were extracted with 300 µL chloroform/methanol (2:1, v/v) for 90–120 min at 4 °C. For neutral lipids analysis, 30 µL of the chloroform phase was subjected to TLC on pre-coated sheets of ALUGRAM Xtra SIL G (Macherey-Nagel, Düren, Germany) using hexane/diethyl ether/acetic acid (90:10:1, $v/v/v$) as the solvent. The resulting spots were compared with those for a mixture of tripalmitin (Merck, Darmstadt, Germany).

2.7. Gas Chromatography-Mass Spectrometry

To determine the total fatty acid (FA) content for each condition showing a spot in the TLC analysis, 5–10 mg of dried whole cells were transmethylated in a single-step method as described in [41], with the following modifications. An internal standard consisting of 100 µL of a 2-br-hexadecanoic acid solution (500 ppm) in toluene was added to each sample for the calculation of the absolute content. Then, 3 mL of a methanol-toluene mixture (4:1 v/v) was added, followed by the addition of 200 µL of acetyl chloride with stirring. Tubes were tightly closed with Teflon-lined caps and subjected to methanolysis at 100 °C for 1 h. After cooling their contents to room temperature, 5 mL of a 6% K_2CO_3 aqueous solution was slowly added. The tubes were subsequently shaken and centrifuged, and the toluene upper phase was extracted and evaporated under nitrogen. Just before chromatographic injection, 100 µL of methyl nonadecanoate (0.5 mg mL^{-1}) was added to the final extracts for a calculation of the recovery relative to that of an internal standard. FA analysis was performed by gas chromatography coupled to mass spectrometry (FOCUS/ISQ II Thermo Fisher Scientific SpA, Milan, Italy/Thermo Fisher Scientific, Austin, TX, USA), using an auto-sampler (TRIPLUS AS3000, Thermo Electron SpA, Milan, Italy) and a ZB23 capillary column (30 m × 0.25 mm internal diameter, 0.25 µm film thickness). A sample volume of 1 µL was injected in the splitless mode (0.8 min). The carrier gas used was He, added at a rate of 1.5 mL min^{-1}. The injector, detector, and transfer line temperatures were 270 °C, 200 °C, and 260 °C, respectively. The mass detector was set to scan mode in a m/w range of 55–400, and the electron energy was set to 70 eV. The oven temperature was programmed at 130 °C for 1 min, raised from 130 °C to 170 °C at a rate of 6.5 °C/min, from 170 °C to 215 °C at a rate of 2.8 °C/min, and subsequently from 215 °C to 230 °C at a rate of 30 °C/min with a 3 min hold. Xcalibur software v2.1.0.1140 was used for instrument control, data acquisition, and analysis. The mass spectra of individual compounds (resolved peaks) were compared with those in the NIST (National Institute of Standards and Technology) library database. FAME quantification was based on the peak area and the response factors of the corresponding standard compound (Supelco™ 37 component FAME Mix, CRM47885, Bellefonte, PA, USA). The FA content was expressed as g/g cellular dry weight (CDW) and the FA profile as the percentage of total FAs present in each specific sample. The quality

of the method was controlled using calibration curves considering a value of $R^2 > 0.99$ as acceptable for individual target compounds.

2.8. Pruning Waste Media Preparation, Chemical Characterization and Conversion to Value-Added Compounds

Fresh or dewatered leaves, obtained by drying leaves in an oven at 40 °C for 24 h, were used to prepare 1 L of olive leaf infusions (named FI and DWI, respectively). Infusions were prepared by boiling 50 g of leaves in 1 L of water for 1 h, adding distilled water to compensate for the evaporation loss. Each infusion was then paper-filtered, autoclaved and pH adjusted to 7. Chemical parameters, including the chemical oxygen demand, total nitrogen and phenol content were quantified using standard methods [42]. Also, the total soluble carbohydrates were determined as described by [43]. The first two parameters were used to estimate the C/N ratio in each medium [44] and determine whether the media could promote neutral lipid accumulation. The growth of *Rhodococcus* sp. 24CO was measured in triplicate at OD600 from samples taken at different times, using uninoculated media as a blank solution. Cultures were collected upon entering the stationary phase and processed as explained in the previous section on neutral lipid accumulation analysis. The intrinsic content of neutral lipids in the olive pruning waste media was also evaluated by thin layer chromatography (TLC), using 1 mL of each waste medium [45]. When a spot was detected, its FA content was quali- and quantitatively analyzed by GC mass spectrometry.

2.9. Transmission Electron Microscopy

Cells used for TEM were fixed overnight in a solution containing 2.5% glutaraldehyde in Sorensen buffer (pH 7.2, final concentration of 0.067 M). Each sample was rinsed twice for 15 min in Sorensen buffer to remove the excess fixative and then post-fixed for 1 h in 2% osmium tetroxide. The samples were washed four times with distilled water for 15 min and then dehydrated in a graded ethanol series (30, 50, 70 and 80 for 15 min, followed by overnight incubation at 96% ethanol). Dehydration continued in 50% acetone/ethanol (*v*/*v*) for 15 min, followed by 100% acetone for 1 h. Samples were then infiltrated with 1:1 Spurr resin/acetone for 1 h, placed in labeled molds filled with 3:1 Spurr resin/acetone mixture, and polymerized at 70 °C overnight. The resulting samples were sectioned at 90 nm using a ultramicrotome with a diamond knife. Thin sections were stained with 2% aqueous uranyl acetate for 1 min and rinsed with distilled water. The dried samples were examined under a JEOL-100 CXII transmission electron microscope (Jeol Ltd., Tokyo, Japan) operating at 80 kV, equipped with a digital camera.

2.10. Oleagenicity Potential of 24CO and Comparison with Model TAG Producers

To further investigate the characteristics of neutral lipid accumulation in *Rhodococcus* sp. 24CO, we compared its genome with the well-studied oleaginous rhodococcal strain *R. jostii* RHA1 using the CD-HIT comparative web server [46]. Sequences were clustered into operational protein units (OPUs) using a sequence identity cutoff of 0.6, as recommended for species within the same genus [47]. After clustering analysis, unique sequences present in RHA1 but absent in strain 24CO, were further considered. In particular, we focused on those whose expression shifted under nitrogen-limited growth conditions in RHA1 based on proteomic [48,49] or transcriptomic studies [50]. Proteins or genes with a +/− two-fold change were considered to detect possible oleagenicity factors. Furthermore, the hypothetical proteins found were subjected to BLAST analysis, and the CDC hits were analyzed to determine potential new functional assignments.

2.11. 24CO Genome Sequence

The sequencing data of the draft genome of *Rhodococcus* sp. 24CO are available online under BioProject PRJNA1070013, NCBI taxonomy ID 3117460 from the NCBI database. This Whole Genome Shotgun project was deposited at DDBJ/ENA/GenBank under the accession number JAZFNF000000000 which corresponds to the version described in this paper.

3. Results

3.1. Isolation and Physiological Features of 24CO

Strain 24CO was obtained from the abaxial side of an Olea europaea var. frantoio leaf together with other bacterial isolates. Once purified, it showed Gram-positive staining with internal refringent inclusions, distinguishing it from the others. The strain was aerobic and formed white, mucoid colonies with a diameter of 3–5 mm when grown on LB agar. It could grow in a range of 4 °C to 30 °C, with an optimal temperature of 28 °C. Examinations of its salinity and pH tolerance showed that 24CO could grow up to 5% *w*/*v* NaCl with a pH that was slightly acidic to basic, ranging from 6 to 10. The strain was able to use a limited number of carbon sources when grown in MSM1 (Figure 1). It showed fast growth with no lag phase in polyols such as mannitol or sorbitol, and fructose (Figure 1A), a short lag phase in some monosaccharides and organic acids (glucose and gluconate, respectively) and a prolonged lag phase in glycerol (Figure 1B). Among the carbon sources tested, the highest OD600 was obtained in fructose. Finally, no growth was observed after 10 days for most of the tested carbon sources, including maltose, lactose, sucrose, xylose and inositol. These results were consistent with those obtained with the API 50CH, which tested the growth on 50 different organic compounds used as carbon sources. *Rhodococcus* sp. 24CO was able to grow only on fructose, mannitol, sorbitol and arabitol (Supplementary Table S1).

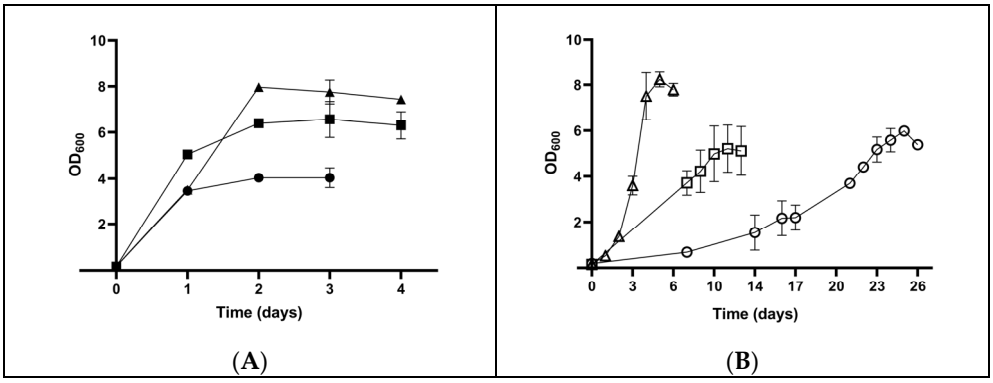

Figure 1. Growth of *Rhodococcus* sp. 24CO on MSM1 measured at an optical density of 600 nm (OD600). (**A**) Fructose 1% (–▲–); mannitol; 1% (–■–) and sorbitol 1% (–●–); (**B**) Glycerol 0.3% *v*/*v* (–o–); glucose 1% (–□–) and gluconate 1% (–Δ–). Unless otherwise stated, prepared in *w*/*v*.

3.2. Genome Analysis

According to BV-BRC annotation, the genome assembly of 24CO yielded 6,603,836 nucleotides in 80 contigs, with a G + C content of 61.7%. It contained 54 RNAs and one copy of a 16S rRNA gene (Table 1). The genome encoded 6560 protein coding sequences (CDS) with 4160 proteins having a functional assignment (1087 proteins found in KEGG pathways), while 2400 were annotated as hypothetical proteins (Table 1). A total of 134 pathways were identified with key metabolic pathways such as those for glycolysis, gluconeogenesis, the glyoxylate cycle, the TCA cycle, the pentose phosphate pathway and fatty acids metabolism being complete. Biosynthesis pathways for amino acids were also present, including those for glutamine, asparagine, serine, cysteine, threonine, tryptophan, leucine, valine, isoleucine, alanine, histidine, phenylalanine, tyrosine, proline, arginine and or-

nithine. Moreover, pathways for the biosynthesis of vitamins such as riboflavin, thiamine and biotin were also assigned. Furthermore, plasmid-like sequences were identified using PLASMe. Among these, proteins associated with mobile genetic elements, such as transposases and proteins associated with conjugation, were found. However, we did not identify complete plasmid sequences. Further studies integrating long-read whole-genome sequencing and Illumina reads will be necessary to determine whether one or more plasmids are present in 24CO. As previously mentioned, the strain was unable to grow on disaccharides (see Section 3.1), and no specific transporters for maltose and lactose were found in the genome. Regarding sucrose metabolism, only the ABC transporter *aglEFG* was present, with no associated transcriptional regulator. Furthermore, the genomic context adjacent to the transporter differed from that usually reported in *Rhodococcus* [20].

Table 1. General features of the *Rhodococcus* sp. 24CO draft genome based on PATRIC platform.

Strain	***Rhodococcus* sp. 24CO**
Domain	*Bacteria*
Taxonomy	*Actinomycetota*; *Actinomycetes*; *Mycobacteriales*; *Nocardiaceae*; *Rhodococcus*
G + C content	61.77
Completeness	99.9
Contamination	0.6
Number of coding sequences (CDSs) in PATRIC	6560
Proteins with functional assignments	4160
Hypothetical proteins	2400
Proteins with EC number assignments	1375
Proteins with KEGG pathway assignments	1087
Number of tRNA	50
Number of rRNA	4
Genome length	6,603,836
N50 value	554,488
L50 value	5

3.3. Phylogenetic Analysis

The phylogenetic tree, calculated using the whole genome information from the TYGS, showed that *Rhodococcus* sp. 24CO clustered on a separate branch from other *Rhodococcus* species, being its closest species, with *R. globerulus* being its closest species (Figure 2). A deeper taxonomic analysis should be performed for a proper phylogenetic assignation of a new species.

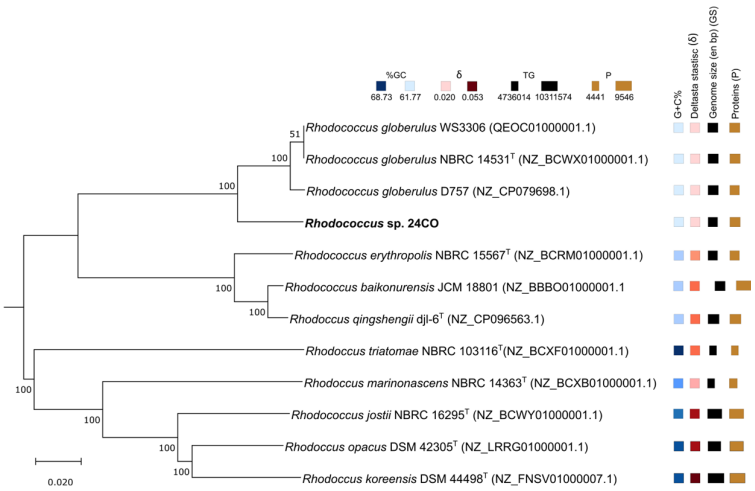

Figure 2. Whole-genome tree constructed using TYGS. Phylogenomic tree was inferred using FASTME 2.1.6.1 and branch support was inferred from 100 pseudobootstrap replicates. Tree was rooted at midpoint. Bootstrap values > 50% are indicated on nodes. Other statistic given by TYGS are also indicated on right side with the corresponding color range or size in the upper part of the Figure.

3.4. Cell Biomass and Synthesis of Neutral Lipids

The ability to produce neutral lipids was analyzed in MSM0.1 using the carbon sources that the strain was able to utilize. Cell biomass production followed a similar pattern to growth, with fructose and mannitol showing the highest values with short harvest times (0.46 g/L and 0.25 g/L, respectively) (Table 2). TLC analysis revealed that *Rhodococcus* sp.

Table 2. Total biomass and valuable compounds obtained using defined substrates from *Rhodococcus* sp. 24CO.

Carbon Source	Harvest Time (h)	Biomass (g CDW/L)	TAG (g/g CDW)
Fructose 1% [a]	48	0.46	0.47
Mannitol 1% [a]	24	0.25	0.28
Sorbitol 1% [a]	24	0.30	0.21
Glucose 1% [a]	240	0.17	0.17
Gluconate 1% [a]	96	0.18	0.19
Glycerol 0.3% [a]	504	0.30	0.23
Mannitol 1% [b]	48	1.49	0.21

[a] MSM0.1. [b] MSM1. CDW, cellular dry weight; TAGs, triacylglycerides.

24CO produced lipids that consisted mainly of the TAGs from every carbon source that supported its growth (Figure 3) GC/MS analysis further confirmed the abundance and FA composition of those TAGs (Figure 4). Considering that a lipid content higher than 20% of the CDW defines a microorganism as oleaginous, the strain reached this criterion for most carbon sources that supported growth. A staggering 7.33 mg of TAGs in 15.5 mg of CDW, representing 47% of the total biomass was detected when the strain was cultivated on MSM 0.1 plus fructose. In addition to fructose, sorbitol, mannitol and glycerol were efficiently converted to TAGs, with a TAG yield of 28% of the CDW with mannitol. Surprisingly, MSM1, i.e., when nitrogen was available, the strain still produced high amounts of neutral lipids with mannitol (Figures 3 and 4 and Table 2). This condition has largely been reported as detrimental to neutral lipid production, promoting growth and biomass production instead. To our knowledge, this is the first report of such behavior. As usually reported for *Rhodococcus*, oleic acid (C18:1) was the most abundant FA, followed by palmitic acid

(C16:0). However, when mannitol was used the composition was dominated by saturated fatty acids (Figure 4).

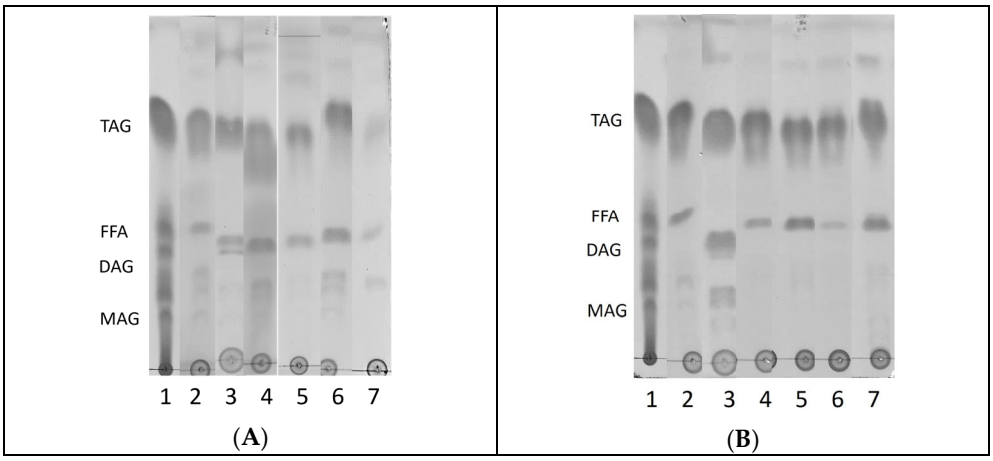

Figure 3. TLC analysis of neutral lipids extracted from 24CO strain grown with different carbon sources. (**A**) MSM1. (**B**) MSM0.1. Lanes: 1. Mixture of neutral lipids used as control: triacylglycerol (TAG), diacylglycerol (DGAT), monoacylglycerol (MAG), free fatty acids (FFAs). 2. Mannitol, 1%. 3. Sorbitol, 1%. 4. Fructose, 1%. 5. Gluconate, 1%. 6. Glucose, 1%. 7. Glycerol, 0.3%.

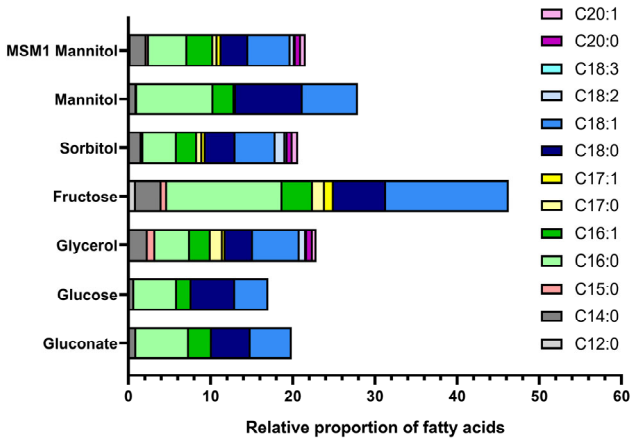

Figure 4. Proportions of fatty acids of TAGs accumulated from different carbon sources. Unless stated otherwise, carbon sources were studied on MSM0.1.

Transmission electron microscopy (TEM) was used to visualize neutral lipid droplets and confirm the high amount of TAGs produced by the strain when it was grown on fructose and mannitol (Supplementary Figure S1). The storage of neutral lipids occurred in inclusions observed to be electron-transparent, round structures that occupied a substantial portion of the cell volume.

3.5. Catabolic Reconstruction for Main Carbon Sources Used by 24CO

TAG synthesis requires precursors and cofactors supplied by various metabolic pathways, primarily those involved in glycolysis, such as the Entner–Doudoroff (ED) pathway, pentose phosphate pathway (PPP) and fatty acid synthesis. Using KEGG, RAST and BV-BRC, we reconstructed the potential metabolic pathway from a carbon source to TAG production (Figure 5). The catabolic pathways for glucose, gluconate and fructose were similar to those that have recently been described [20]. Natural polyols, found in its free form, have never been studied in *Rhodococcus*. Therefore, we focused on these carbon sources, which are abundant in olive leaves. The genome analysis of 24CO revealed two putative polyols transporters, which we named *smoEFGK*a and *smoEFGK*b. Furthermore,

mannitol and sorbitol appeared to share the same transporter, being internalized via the polyol ABC transporter, *smoEFGK*a, which exhibited homology to *smoKGFE* from *Mycobacterium smegmatis* [47]. Interestingly, upstream of this transporter we identified genes encoding (i) the transcriptional regulator *smoR*, (ii) sorbitol-2-dehydrogenase SORD, and (iii) mannitol-2-dehydrogenase *mtlK*. Downstream of the ABC transporter, we found a fructokinase (*scrK*) gene (Figure 5). A second ABC transporter (*smoEFGK*b) that could be involved in polyol metabolism, was also identified. It has a similar topology to *smoEFGK*a but lacked *mtlK* and *scrK*. MtlK and SORD are likely involved in converting their respective polyols to fructose. As an intermediary in this pathway, fructose can enter the Embden-Meyerhof-Parnas pathway (EM) after phosphorylation to fructose 6-phosphate by *scrK* or be directed to the PPP if converted into glucose 6-phosphate (Figure 5).

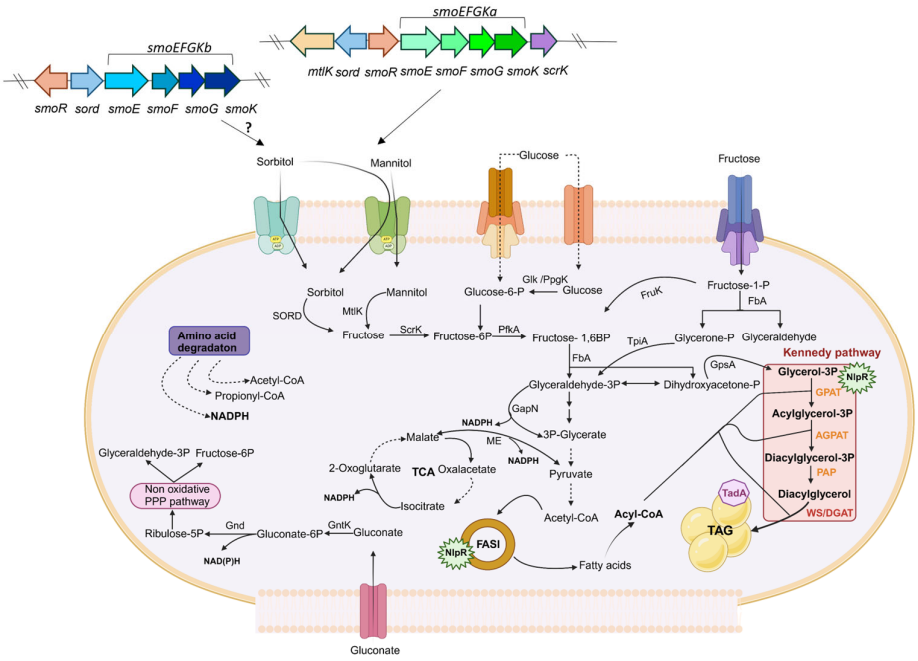

Figure 5. Reconstruction of metabolic pathway from carbon source to TAG production in strain 24CO. TCA: tricarboxylic acid cycle; PPP: pentose phosphate pathway; TAG: triacylglycerol; FASI: fatty acid biosynthesis; GntK: Gluconokinase; Gnd: 6-phosphogluconate-dehydrogenase; Glk: Glucokinase; PpgK: polyphosphateglucose phosphotransferase; SORD: sorbitol-2-dehydrogenase; MtlK: mannitol-2-dehydrogenase; Pgi: glucose 6-phosphate-isomerase; Scrk: fructokinase; FruK: 1-phosphofructokinase; TpiA: triose bisphosphate isomerase; FbA: fructose bisphosphate aldolase; GpsA: NADP-dependent glycerol-3-phosphate dehydrogenase; GapN: nonphosphorylating glyceraldehyde-3-phosphate dehydrogenase; Gnd: 6-phosphogluconate dehydrogenase; Pfk: ATP-dependent phosphofructokinase/diphosphate-dependent phosphofructokinase; ME: malic enzyme; ICDH: NADP-dependent isocitrate dehydrogenase; GPAT: glycerol-3-phosphate acyltransferase; AGPAT: acylglycerolphosphate acyltransferase; PAP: phosphatidic acid phosphatase enzyme; WS/DGAT: wax ester/diacylglycerol acyltransferase; TadA: major lipid droplet protein; NlpR: nitrogen lipid regulator.

Among the glycolytic pathways, the EM route responsible for generating pyruvate and acyl-CoA for fatty acid biosynthesis was complete, whereas the genes necessary for the Entner–Doudoroff pathway were absent. The PPP was also present, supplying the reductive power required for fatty acid biosynthesis. Additionally, genes encoding proteins related to oleagenicity, such as GapN (glyceraldehyde-3-phosphate dehydrogenase), GpsA (NADP-dependent glycerol-3-phosphate dehydrogenase), NlpR (nitrogen lipid regulator), NADPH-dependent malic enzyme, and TadA (major lipid droplet protein), were identified in the genome. Furthermore, genes involved in amino acid degradation which produced acetyl-CoA, propionyl-CoA and NADPH, essential for fatty acid biosynthesis, were also detected.

Finally, the Kennedy pathway for TAG biosynthesis was complete, with a high redundancy for most enzymes involved in the process (Figure 5 and Supplementary Table S2).

3.6. Agricultural Waste Revalorization

Rhodococcus sp. 24CO was able to convert olive pruning waste into valuable lipids, producing more than 20% of the CDW in the DWI and 8% in the FI (Figure 6). Different chemical parameters that could influence neutral lipid accumulation were analyzed in both the FI and the DWI (Table 3). Based on the obtained values, both infusions were suitable candidates for lipid production due to their high C/N ratios. The total sugar concentration, approximately 20 g L^{-1}, was similar in both media tested. The extractable phenol concentration in water was low for both waste sources. The total lipid content reached 1.8%, with linolenic acid (C18:3) as the major component. *Rhodococcus* sp. 24CO was able to grow in both media, displaying similar dynamics in its growth curves (Figure 6A) but showing higher values for the cell biomass for the DWI in comparison to the FI (0.18 g CDW/L and 0.08 g CDW/L, respectively). Neutral lipid accumulation varied between the two residues, with the DWI yielding over 20% of the CDW compared to an 8% yield in the FI (Figure 6B). In terms of the TAG composition, the FI primarily demonstrated the classic C18:1/C16:0 profile, whereas the 20% obtained from the DWI resembled the composition observed for mannitol (Figure 6B). Additionally, a small amount of polyhydroxybutyrate (PHB) was detected in both cases. The genome analysis of *Rhodococcus* sp. 24CO further revealed its potential for synthesizing these polymers (Supplementary Table S3).

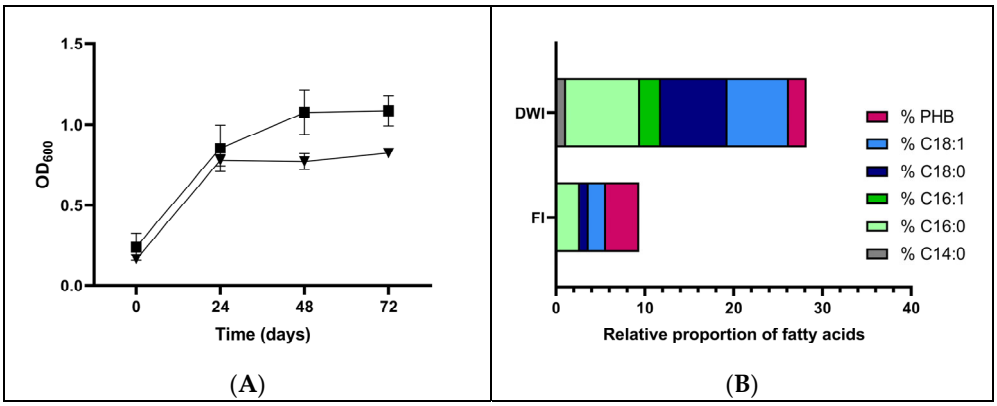

Figure 6. Growth and TAG accumulation results for Fresh Infusion (FI) and Dewatered Infusion (DWI). (**A**) Growth of strain 24CO in both media (–▼–: FI; –■–: DWI). (**B**) Relative proportion of fatty acids in TAGs or PHB by cellular dry weight.

Table 3. Chemical parameters for each infusion prepared from pruning waste.

	COD (mg/L)	Total Nitrogen (mg/L)	C/N Ratio	Total Sugar (g/L)	Phenol Content (mg/L)
Fresh Infusion (FI)	29,550	119	248.3	21.0	5.8
Dewatered Infusion (DWI)	7410	29	255.5	19.9	2.7

3.7. Oleagenicity

Rhodococcus sp. 24CO was able to grow on gluconate. However, it produced low amounts of neutral lipids (<20% of CDW) (Figure 4). In contrast, oleaginous strains such as *R. jostii* RHA1 could reach a TAG yield of up to 76% of their CDW when grown on this carbon source. Available data from transcriptomic and proteomic studies of *R. jostii RHA1* grown in MSM0.1 with gluconate were used to detect those genes/proteins relevant to the process (up- or downregulated) that were absent in strain 24CO (Supplementary Table S4).

This comparative analysis had never before been used to unravel the factors that result in an oleaginous phenotype. It also provided insight into those genes that were relevant or irrelevant for oleagenicity in 24CO, according to the carbon source used. After a CD-HIT clustering analysis, a total of 562 genes/proteins from RHA1 shifted in conditions favoring neutral lipid accumulation. Only 244 proteins had a functional annotation, and the rest were annotated as hypothetical proteins. Upregulated proteins included enzymes belonging to the Entner–Doudoroff (ED) pathway and a wax ester/triacylglycerol synthase family O-acyltransferase (WS/DGAT). Transcriptomic analysis revealed a wider spectrum of genes absent in 24CO. Among them, different transporters (for ions: Cu^{+2}, Fe^{+3} or not specified), putative genes implicated in redox metabolism (kinase, dehydrogenase and oxidoreductase genes) and 23 putative transcriptional regulators, along with two universal stress proteins (RS00325 and RS00165), were detected. In addition, genes related to lipid metabolism were identified, including acyl-CoA binding protein, acyl-CoA dehydrogenase, long-chain fatty acyl-CoA ligase, TAG lipase, 3-oxoacyl-[acyl carrier protein] reductase, enoyl-CoA hydratase, 3-hydroxyacyl-CoA dehydrogenase and two WS/DGATs. On the other hand, 49 downregulated genes were found, such as those encoding NADPH/NADH-dependent dehydrogenases, genes associated with amino acid metabolism, transporters and six transcriptional regulators. Proteomic analysis revealed that of 19 proteins absent in 24CO, 17 of them were upregulated and 3 of them were directly implicated in TAG metabolism, an enoyl-CoA hydratase (RS13930), an acyl-ACP desaturase (RS28630) and a wax ester/triacylglycerol synthase family O-acyltransferase (RS07790). Furthermore, one transcriptional regulator (RS10400) and three genes associated with nitrogen metabolism were found. Among their downregulated counterparts, an ABC transporter (RS27545) and glyceraldehyde-3-phosphate dehydrogenase (RS16630) were identified.

4. Discussion

In this work, we have described the isolation of *Rhodococcus* sp. 24CO from olive leaves and characterized its growth in pruning waste with different unique carbon sources that resulted in the production of polymeric and non-polymeric neutral lipids. Through phyllosphere studies, epiphytic Actinobacteria and representatives of the *Rhodococcus* genus, closely related to *R. fascians* and *R. corynebacteroides*, have been identified in olive leaf communities [11,51]. These studies have focused on the ecological role or taxonomic affiliation of the bacterial isolates rather than their possible biotechnological applications such as neutral lipid storage. The *Rhodococcus* genus has been widely studied in relation to this biotechnological process, which interests different industries [14,18]. Beyond phenolic compounds, olive leaves contain other metabolites that can serve as a carbon source [52]. Olive pruning waste is an agro-industrial by-product that has been scarcely explored as raw material to produce commercially relevant compounds from bacteria. To our knowledge, there has only been one report that shows its value for PHB accumulation by *Cobetia amphilecti* [53]. In this study, the production of neutral lipids from pruning waste was explored for the first time. *Rhodococcus* sp. 24CO exhibited high levels of neutral lipid accumulation when grown on this substrate, highlighting the value of this combination of bacteria and a by-product. Previous reports of olive waste have primarily focused on oil mill waste, where different *Rhodococcus* species demonstrated strong growth as well as TAG accumulation or biosurfactant production [54,55]. Interestingly, none of these studies indicated the accumulation of PHB, while 24CO showed the potential to produce this polyester from infusions prepared from olive leaf extracts. This highlights the relevance of pruning waste for PHB production. When comparing both infusions, the DWI waste proved to be a better substrate than the FI for biomass production and the lipid yield. The lower content of toxic compounds such as phenols may explain the differences in growth.

TAG accumulation was also higher in the DWI over than the FI, possibly due to the low nitrogen content in the DWI. The production of TAGs by 24CO from olive pruning waste represents a novel biotechnological application of this strain, helping to mitigate the large amount of waste generated during pruning. It is also relevant that linolenic acid (C18:3) was the main fatty acid present in olive leaves, in accordance with previous reports [56,57] but, apparently it was not incorporated into bacterial TAGs. The metabolic pathways involved in TAG synthesis in *Rhodococcus* have been deeply studied (reviewed in [58]). While the ability to synthesize and accumulate neutral lipids in *R. globerulus* is unknown, *R. erythropolis* has been extensively studied regarding neutral lipid synthesis from classical carbon sources and agro-industrial waste [20,59]. Olive leaves contain mannitol as one of their most abundant soluble nutrients and fructose [22,23]. *Rhodococcus* sp. 24CO showed a similar growth dynamic to *R. erythropolis* when cultivated with fructose, gluconate or glucose as the only carbon source. Unfortunately, no previous reports showing biomass yields with classic and unique carbon sources were published with which to compare our findings. Interestingly, when the carbon source was fructose, strain 24CO showed higher TAG accumulation in comparison to *R. erythropolis* and model oleaginous *Rhodococcus* species such as *R. opacus* PD630 or *R. jostii* RHA1 [20,60]. Regarding polyols, this is the first work that shows the relevance of these compounds as carbon sources and how they impact bacterial neutral lipid accumulation. Along with fructose, polyols were the most efficient carbon source for neutral lipid production. This preference could be related to the chemical composition of olive leaves, from which the strain was originally isolated. On the other hand, 24CO was unable to grow on disaccharides, likely due to the absence of putative maltose and lactose transporters like those reported in *Streptomyces coelicolor* and *Rhodococcus* [61,62]. For sucrose, 24CO contained the same putative transporter as that reported for RHA1 [20]. However, the transcriptional regulator adjacent to it was absent. Thus, it could be hypothesized that the strain cannot grow on disaccharides because it lacks transporters or regulators that orchestrate their internalization. With all carbon sources used, the greatest proportions of fatty acid were assigned to C16:0, C18:0 and C18:1, consistent with the classic composition reported for *Rhodococcus* [63,64]. The most striking result was the efficiency of TAG accumulation when strain 24CO was grown on nitrogen rich media. Typically, an oleaginous phenotype requires a high C/N ratio, which promotes neutral lipid accumulation at the expense of growth [60]. Surprisingly, the strain accumulated more than a 20% content of TAGs when nitrogen was plentiful available. This finding is novel and industrially relevant since the strain would produce a high biomass and, simultaneously, high amounts of TAGs.

Among the pathways reported to be involved in TAG synthesis, *Rhodococcus* sp. 24CO presented almost all of them, except the ED pathway. Reports on oleaginous *Rhodococcus* have shown that the ED pathway is a very active and important pathway in oleaginous *Rhodococcus* when grown on gluconate or glucose [48–50]. Its absence in strain 24CO may explain its poor performance when utilizing these carbon sources. Fructose represented the best carbon source for neutral lipid accumulation in *Rhodococcus* sp. 24CO. There are no reports on the specific metabolic pathways involved in fructose metabolism in *Rhodococcus*. Based on our results, the absence of the ED pathway does not appear to hinder TAG synthesis. There was also no prior information on the pathways responsible for polyol internalization and metabolism in *Rhodococcus*, but the genomic context in strain 24CO closely resembles that reported in *Mycobacterium* and *Sinorhizobium* [47,65]. In strain 24CO, we found two putative transporters for polyols, *smoEFGK*a and *smoEFGK*b. Interestingly, adjacent to *smoEFGK*a, we found genes implicated in the subsequent metabolism of polyols, as was demonstrated for *Sinorhizobium meliloti* [65]. Regarding *smoEFGK*b, a SORD gene was found between the regulator *smoR* and *smoE*. These same genes are found on

Alphaproteobacteria but with a different gene arrangement in comparison with the cluster we found [66]. As reported by [65], mannitol (or sorbitol) would probably be further converted to fructose through the action of two consecutive reactions catalyzed by *mtlK* (or SORD) and *scrK*, further followed by fructose metabolism. The understanding of the metabolic aspects that make some *Rhodococcus* strains oleaginous and not others, under similar growth conditions, is absolutely relevant in this field. This could not only improve our knowledge of neutral lipid accumulation, but it may also help to identify key gene players for enhancing these biotechnological lipid factories. The *Rhodococcus* sp. 24CO genome contains fewer than half of the 16 *ws/dgat* present in RHA1 [67]. However, they were sufficient for achieving the highest values of TAG accumulation obtained in fructose, even surpassing those of the well-established oleaginous rhodococcal strains. Moreover, the enzymes and regulators of the ED pathway upregulated in omics analyses of *R. jostii* RHA1 [48–50] but absent in 24CO may suggest that this route is not involved in fructose or mannitol catabolism and subsequent TAG accumulation. The relevance of this pathway lies in its production of NADPH, required for fatty acid biosynthesis (reviewed in [58]). As strain 24CO lacks the ED pathway, the reductive power could be supplied by the PP pathway. How the strain copes with the excess of sugar–phosphate intermediaries, usually channeled through the ED pathway, remains to be studied. Furthermore, *Rhodococcus* sp. 24CO also lacks genes associated with redox metabolism, such as those encoding dehydrogenases and oxidoreductases, which are often involved in the generation of the NADPH or NADH necessary for oleaginous metabolism [50]. Genes associated with fatty acid biosynthesis, elongation or degradation were detected in 24CO. However, these were not the same copies as those upregulated in RHA1, constituting another feature that could define an oleaginous *Rhodococcus* (at least when grown in gluconate). Additionally, key genes upregulated in RHA1 associated with nitrogen metabolism, such as nitrite reductase or urease, were not found in 24CO. Whether the lack of these or other nitrogen cycle-related genes contributes to shaping an oleaginous phenotype in balanced C/N growth conditions remains to be studied. Moreover, 24CO did not exhibit stress proteins and transcriptional regulators, whose expression is driven by nitrogen limitation in RHA1 [48,67]. This result could explain the unexpected ability to accumulate neutral lipids when nitrogen is available, a condition that usually does not induce considerable TAG storage. Also, there were two WS/DGATs upregulated in the transcriptome and proteome analysis which did not have homology to any of the seven WS/DGATs found in the 24CO strain. Whether these enzymes are important for gluconate but not relevant for TAG accumulation when polyols or fructose are used as a carbon source could be determined through future experiments.

5. Conclusions

The global need to recycle agro-industrial by-products into valuable compounds is urgent, particularly for toxic waste that contributes to environmental pollution. The use of environmental microbes could help us to find a solution. Also, their exceptional capacity to tolerate and adapt to extreme environmental conditions through the synthesis and accumulation of neutral lipids (TAGs) make them attractive candidates for bio-based production. In this work, we used a novel microbial approach and demonstrated that *Rhodococcus* sp. 24CO, isolated from the olive phyllosphere, is a valuable strain. It could efficiently use agro-industrial waste, such as olive pruning leaves, for the production of value-added compounds including TAGs and, to a lesser extent, PHB. It is also able to metabolize natural carbon sources, such as fructose or polyols, showing a strong preference for these metabolites found in olive leaves. This growth behavior suggests a strong adaptation to its natural environment. An unprecedent result presented in this work is the capacity of 24CO to accu-

mulate large amounts of TAGs even under nitrogen-rich conditions. The metabolic context and regulatory mechanisms for lipid synthesis in 24CO require further investigation.

In future work, we will focus on the genetic and enzymatic mechanisms that govern lipid accumulation in 24CO, particularly in relation to polyol metabolism. Mannitol/sorbitol metabolism and their genetic determinants have never been studied in *Rhodococcus* and deserve deeper study. Omics studies could help identify key metabolic regulators, transporters and metabolic pathways that could potentially help us to understand the strain's behavior, which differs from that of the oleaginous model strain *R. jostii* RHA1. Additionally, a long-term goal relates to exploring the potential for scaling up TAG and PHB production using olive pruning waste, considering bioprocess optimization.

Finally, *Rhodococcus* sp. 24CO represents a promising microbial platform for sustainable lipid production. However, much work is needed to understand its behavior and the metabolic traits that make it unique.

Supplementary Materials: The following supporting information can be downloaded at: https://www.mdpi.com/article/10.3390/fermentation11050237/s1, Figure S1: TEM images of 24CO strain grown in conditions favoring neutral lipid accumulation; Table S1: Results from API50CH for *Rhodococcus* sp. 24CO; Table S2: Set of genes associated with biosynthesis of TAGs in *Rhodococcus* sp. 24CO; Table S3: Set of genes associated with PHA metabolism in *Rhodococcus* sp. 24CO; Table S4: Set of genes absent in *Rhodococcus* sp. 24CO and shifted in omic studies of *R. jostii* RHA1.

Author Contributions: Conceptualization, M.P.L.; methodology, M.P.L. and M.G.; software, N.E.S.; validation, N.E.S. and M.P.L.; formal analysis, N.E.S.; investigation, N.E.S.; resources, M.P.L., N.S.A. and M.G.; data curation, N.E.S.; writing—original draft preparation, M.P.L. and N.E.S.; writing—review and editing, M.G., N.S.A. and H.M.A.; visualization, N.E.S.; supervision, M.P.L.; project administration, M.P.L.; funding acquisition, H.M.A. All authors have read and agreed to the published version of the manuscript.

Funding: This study was financially supported by PUE2018-INBIOP 0033 (CONICET, Argentina) and PICT2020 Serie A Nro. 02215 (ANPCyT, Argentina).

Institutional Review Board Statement: Not applicable.

Informed Consent Statement: Not applicable.

Data Availability Statement: All data are accessible as stated in the main text. Any further inquiries can be directed to the corresponding author.

Acknowledgments: We would like to thank Joseph A. Christie-Oleza for carefully reading the manuscript and Ing. Marcos A. Franco from IPEEC CENPAT for his technical assistance in GC data acquisition. N.E.S. is a CONICET doctorate fellowship recipient. M.P.L., N.S.A. and H.M.A. are CONICET career researchers.

Conflicts of Interest: The authors declare no conflicts of interest.

References

1. Zopf, W. Über Ausscheidung von Fettfarbstoffen (Lipochromen) seitens gewisser Spaltpilze. *Ber. Dtsch. Bot. Ges.* **1891**, *9*, 22–28.
2. Cappelletti, M.; Zampolli, J.; Di Gennaro, P.; Zannoni, D. Genomics of Rhodococcus. In *Biology of Rhodococcus*; Alvarez, H.M., Ed.; Springer: Cham, Switzerland, 2019; pp. 23–60. [CrossRef]
3. Ruberto, L.A.; Vazquez, S.; Lobalbo, A.; Mac Cormack, W.P. Psychrotolerant hydrocarbon-degrading *Rhodococcus* strains isolated from polluted Antarctic soils. *Antarct. Sci.* **2005**, *17*, 47–56. [CrossRef]
4. Silva, R.A.; Grossi, V.; Olivera, N.L.; Alvarez, H.M. Characterization of indigenous *Rhodococcus* sp. 602, a strain able to accumulate triacylglycerides from naphthyl compounds under nitrogen-starved conditions. *Res. Microbiol.* **2010**, *161*, 198–207. [CrossRef] [PubMed]
5. Wilson, M.; Lindow, S.E. Coexistence among epiphytic bacterial populations mediated through nutritional resource partitioning. *Appl. Environ. Microbiol.* **1994**, *60*, 4468–4477. [CrossRef]

6. Kirkwood, R.C. Recent developments in our understanding of the plant cuticle as a barrier to the foliar uptake of pesticides. *Pestic. Sci.* **1999**, *55*, 69–77. [CrossRef]
7. Koskella, B. The phyllosphere. *Cur. Biol.* **2020**, *30*, R1143–R1146. [CrossRef]
8. Stone, B.W.; Weingarten, E.A.; Jackson, C.R. The Role of the Phyllosphere Microbiome in Plant Health and Function. *Annu. Rev. Plant Biol.* **2018**, *1*, 533–556. [CrossRef]
9. Chaudhary, D.; Kumar, R.; Sihag, K.; Kumari, A. Phyllospheric microflora and its impact on plant growth: A review. *Agric. Rev.* **2017**, *38*, 51–59. [CrossRef]
10. Kämpfer, P.; Wellner, S.; Lohse, K.; Lodders, N.; Martin, K. *Rhodococcus cerastii* sp. nov. and *Rhodococcus trifolii* sp. nov., two novel species isolated from leaf surfaces. *Int. J. Syst. Evol. Microbiol.* **2013**, *63 Pt 3*, 1024–1029. [CrossRef]
11. Dhaouadi, S.; Mougou, A.H.; Wu, C.J.; Gleason, M.L.; Rhouma, A. Sequence analysis of 16S rDNA, *gyrB* and *alkB* genes of plant-associated *Rhodococcus* species from Tunisia. *Int. J. Syst. Evol. Microbiol.* **2020**, *70*, 6491–6507. [CrossRef]
12. Crombie, A.T.; Larke-Mejia, N.L.; Emery, H.; Dawson, R.; Pratscher, J.; Murphy, G.P.; McGenity, T.J.; Murrell, J.C. Poplar phyllosphere harbors disparate isoprene-degrading bacteria. *Proc. Natl. Acad. Sci. USA* **2018**, *115*, 13081–13086. [CrossRef] [PubMed]
13. Sandhu, A.; Halverson, L.J.; Beattie, G.A. Identification and Genetic Characterization of Phenol-Degrading Bacteria from Leaf Microbial Communities. *Microb. Ecol.* **2009**, *57*, 276–285. [CrossRef] [PubMed]
14. Alvarez, H.M.; Hernández, M.A.; Lanfranconi, M.P.; Silva, R.A.; Villalba, M.S. *Rhodococcus* as biofactories for microbial oil production. *Molecules* **2021**, *26*, 4871. [CrossRef] [PubMed]
15. Pátek, M.; Grulich, M.; Nešvera, J. Stress response in *Rhodococcus* strains. *Biotechnol. Adv.* **2021**, *53*, 107698. [CrossRef]
16. Huang, J.; Ai, G.; Liu, N.; Huang, Y. Environmental Adaptability and Organic Pollutant Degradation Capacity of a Novel *Rhodococcus* Species Derived from Soil in the Uninhabited Area of the Qinghai-Tibet Plateau. *Microorganisms* **2022**, *10*, 1935. [CrossRef]
17. Ghosh, A.; Khurana, M.; Chauhan, A.; Takeo, M.; Chakraborti, A.; Jain, R. Degradation of 4-nitrophenol, 2-chloro-4-nitrophenol, and 2,4-dinitrophenol by *Rhodococcus imtechensis* strain RKJ300. Environ. *Sci. Technol.* **2010**, *44*, 1069–1077. [CrossRef]
18. Cappelletti, M.; Presentato, A.; Piacenza, E.; Firrincieli, A.; Turner, R.J.; Zannoni, D. Biotechnology of *Rhodococcus* for the production of valuable compounds. *Appl. Environ. Microbiol.* **2020**, *104*, 8567–8594. [CrossRef]
19. Bequer Urbano, S.; Albarracín, V.H.; Ordoñez, O.F.; Farías, M.E.; Alvarez, H.M. Lipid storage in high-altitude Andean Lakes extremophiles and its mobilization under stress conditions in *Rhodococcus* sp. A5, a UV-resistant actinobacterium. *Extremophiles* **2013**, *17*, 217–227. [CrossRef]
20. Herrero, O.M.; Alvarez, H.M. Fruit residues as substrates for single-cell oil production by *Rhodococcus* species: Physiology and genomics of carbohydrate catabolism. *World J. Microbiol. Biotechnol.* **2024**, *40*, 61. [CrossRef]
21. Hosseini, S.V.; Dastgerdi, H.E.; Tahergorabi, R. Marine Mannitol: Extraction, Structures, Properties, and Applications. *Processes* **2024**, *12*, 1613. [CrossRef]
22. Medina, E.; Romero, C.; García, P.; Brenes, M. Characterization of bioactive compounds in commercial olive leaf extracts, and olive leaves and their infusions. *Food Funct.* **2019**, *10*, 4716–4724. [CrossRef] [PubMed]
23. Gomez-Gonzalez, S.; Ruiz-Jimenez, J.; Priego-Capote, F.; Luque de Castro, M.D. Qualitative and quantitative sugar profiling in olive fruits, leaves, and stems by gas chromatography-tandem mass spectrometry (GC-MS/MS) after ultrasound-assisted leaching. *J. Agric. Food Chem.* **2010**, *58*, 12292–12299. [CrossRef] [PubMed]
24. Pharr, D.M.; Stoop, J.M.H.; Williamson, J.D.; Studer Feusi, M.E.; Massel, M.O.; Conkling, M.A. The dual role of mannitol as osmoprotectant and photoassimilate in celery. *Hortic. Sci.* **1995**, *30*, 1182–1188. [CrossRef]
25. Arias, N.S.; Scholz, F.G.; Goldstein, G.; Bucci, S. The cost of avoiding freezing in stems: Trade-off between xylem resistance to cavitation and supercooling capacity in woody plants. *Tree Physiol.* **2017**, *37*, 1251–1262. [CrossRef]
26. Galliou, F.; Markakis, N.; Fountoulakis, M.S.; Nikolaidis, N.; Manios, T. Production of Organic Fertilizer from Olive Mill Wastewater by Combining Solar Greenhouse Drying and Composting. *Waste Manag.* **2018**, *75*, 305–311. [CrossRef]
27. Mira-Urios, M.Á.; Sáez, J.A.; Orden, L.; Marhuenda-Egea, F.C.; Andreu-Rodríguez, F.J.; Toribio, A.J.; Agulló, E.; López, M.J.; Moral, R. Composting of Olive Mill Wastewater Sludge Using a Combination of Multiple Strategies: Assessment of Improvement in Biodegradability, GHG Emissions, and Characteristics of the End Product. *Agronomy* **2025**, *15*, 808. [CrossRef]
28. Roig, A.; Cayuela, M.L.; Sánchez-Monedero, M.A. An overview on olive mill wastes and their valorisation methods. *Waste Manag.* **2006**, *26*, 960–969. [CrossRef]
29. Enaime, G.; Dababat, S.; Wichern, M.; Lübken, M. Olive mill wastes: From wastes to resources. *Environ. Sci. Pollut. Res.* **2024**, *31*, 20853–20880. [CrossRef]
30. Espeso, J.; Isaza, A.; Lee, J.Y.; Sörensen, P.M.; Jurado, P.; Avena-Bustillos, R.D.J.; Olaizola, M.; Arboleya, J.C. Olive leaf waste management. *Front. Sustain. Food Syst.* **2021**, *5*, 660582. [CrossRef]
31. Schlegel, H.G.; Kaltwasser, H.; Gottschalk, G. Ein Submersverfahren zur Kultur wasserstoffoxydierender Bakterien: Wachstumsphysiologische Untersuchungen. *Arch. Mikrobiol.* **1961**, *38*, 209–222. [CrossRef]

32. Bolger, A.M.; Lohse, M.; Usadel, B. Trimmomatic: A flexible trimmer for Illumina Sequence Data. *Bioinformatics* **2014**, *30*, 2114–2120. [CrossRef] [PubMed]
33. Bushnell, B. BBTools Software Package. 2014. Available online: https://sourceforge.net/projects/bbmap/ (accessed on 27 June 2022).
34. Arkin, A.P.; Cottingham, R.W.; Henry, C.S.; Harris, N.L.; Stevens, R.L.; Maslov, S.; Dehal, P.; Ware, D.; Perez, F.; Canon, S.; et al. KBase: The United States department of energy systems biology knowledgebase. *Nat. Biotechnol.* **2018**, *36*, 566–569. [CrossRef] [PubMed]
35. Aziz, R.K.; Bartels, D.; Best, A.A.; DeJongh, M.; Disz, T.; Edwards, R.A.; Formsma, K.; Gerdes, S.; Glass, E.M.; Kubal, M.; et al. The RAST Server: Rapid annotations using subsystems technology. *BMC Genom.* **2008**, *9*, 75. [CrossRef]
36. Olson, R.D.; Assaf, R.; Brettin, T.; Conrad, N.; Cucinell, C.; Davis, J.J.; Dempsey, D.M.; Dickerman, A.; Dietrich, E.M.; Kenyon, R.W.; et al. IIntroducing the Bacterial and Viral Bioinformatics Resource Center (BV-BRC): A resource combining PATRIC, IRD and ViPR. *Nucleic Acids Res.* **2023**, *51*, D678–D689. [CrossRef] [PubMed]
37. Tang, X.; Shang, J.; Ji, Y.; Sun, Y. PLASMe: A tool to identify PLASMid contigs from short-read assemblies using transformer. *Nucleic Acids Res.* **2023**, *51*, e83. [CrossRef]
38. Meier-Kolthoff, J.P.; Göker, M. TYGS is an automated high-throughput platform for state-of-the-art genome-based taxonomy. *Nat. Commun.* **2019**, *10*, 2182. [CrossRef]
39. Moriya, Y.; Itoh, M.; Okuda, S.; Yoshizawa, A.; Kanehisa, M. KAAS: An automatic genome annotation and pathway reconstruction server. *Nucleic Acids Res.* **2007**, *35*, W182–W185. [CrossRef]
40. Ceniceros, A.; Dijkhuizen, L.; Petrusma, M.; Medema, M.H. Genome-based exploration of the specialized metabolic capacities of the genus *Rhodococcus*. *BMC Genom.* **2017**, *18*, 593. [CrossRef]
41. Lepage, G.; Roy, C.C. Direct transesterification of all classes of lipids in a one-step reaction. *J. Lipid Res.* **1986**, *27*, 114–120. [CrossRef]
42. Rice, E.W.; Baird, R.; Eaton, A.D.; Bridgewater, L. *Standard Methods for the Examination of Water and Wastewater*, 22nd ed.; American Public Health Association: Washington, DC, USA, 2012.
43. DuBois, M.; Gilles, K.A.; Hamilton, J.K.; Rebers, P.T.; Smith, F. Colorimetric method for determination of sugars and related substances. *Anal. Chem.* **1956**, *28*, 350–356. [CrossRef]
44. Cheirsilp, B.; Louhasakul, Y. Industrial wastes as a promising renewable source for production of microbial lipid and direct transesterification of the lipid into biodiesel. *Biores. Technol.* **2013**, *142*, 329–337. [CrossRef] [PubMed]
45. Villalba, M.S.; Alvarez, H.M. Identification of a novel ATP-binding cassette transporter involved in long-chain fatty acid import and its role in triacylglycerol accumulation in *Rhodococcus jostii* RHA1. *Microbiology* **2014**, *160*, 1523–1532. [CrossRef] [PubMed]
46. Ying, H.; Beifang, N.; Ying, G.; Limin, F.; Weizhong, L. CD-HIT Suite: A web server for clustering and comparing biological sequences. *Bioinformatics* **2010**, *26*, 680–682. [CrossRef]
47. Titgemeyer, F.; Amon, J.; Parche, S.; Mahfoud, M.; Bail, J.; Schlicht, M.; Rehm, N.; Hillmann, D.; Stephan, J.; Walter, B.; et al. A genomic view of sugar transport in *Mycobacterium smegmatis* and *Mycobacterium tuberculosis*. *J. Bacteriol.* **2007**, *189*, 5903–5915. [CrossRef] [PubMed]
48. Dávila Costa, J.S.; Herrero, O.M.; Alvarez, H.M.; Leichert, L. Label-free and redox proteomic analyses of the triacylglycerol-accumulating *Rhodococcus jostii* RHA1. *Microbiology* **2015**, *161 Pt 3*, 593–610. [CrossRef]
49. Dávila Costa, J.S.; Silva, R.A.; Leichert, L.; Alvarez, H.M. Proteome analysis reveals differential expression of proteins involved in triacylglycerol accumulation by *Rhodococcus jostii* RHA1 after addition of methyl viologen. *Microbiology* **2017**, *163*, 343–354. [CrossRef]
50. Juarez, A.; Villa, J.A.; Lanza, V.F.; Lázaro, B.; de la Cruz, F.; Alvarez, H.M.; Moncalián, G. Nutrient starvation leading to triglyceride accumulation activates the Entner Doudoroff pathway in *Rhodococcus jostii* RHA1. *Microb. Cell Factories* **2017**, *16*, 35. [CrossRef]
51. Mina, D.; Pereira, J.A.; Lino-Neto, T.; Baptista, P. Epiphytic and endophytic bacteria on olive tree phyllosphere: Exploring tissue and cultivar effect. *Microb. Ecol.* **2020**, *80*, 145–157. [CrossRef]
52. Guodong, R.; Xiaoxia, L.; Weiwei, Z.; Wenjun, W.; Jianguo, Z. Metabolomics reveals variation and correlation among different tissues of olive (*Olea europaea* L.). *Biol. Open* **2017**, *6*, 1317–1323. [CrossRef]
53. Gnaim, R.; Unis, R.; Gnayem, N.; Das, J.; Gozin, M.; Golberg, A. Turning mannitol-rich agricultural waste to poly (3-hydroxybutyrate) with *Cobetia amphilecti* fermentation and recovery with methyl levulinate as a green solvent. *Biores. Technol.* **2022**, *352*, 127075. [CrossRef]
54. Herrero, O.M.; Villalba, M.S.; Lanfranconi, M.P.; Alvarez, H.M. *Rhodococcus* bacteria as a promising source of oils from olive mill wastes. *World J. Microbiol. Biotechnol.* **2018**, *34*, 114. [CrossRef] [PubMed]
55. Negrete, P.S.; Ghilardi, C.; Pineda, L.R.; Pérez, E.; Herrera, M.L.; Borroni, V. Biosurfactant Production by *Rhodococcus* ALDO1 Isolated from Olive Mill Wastes. *Biocatal. Agric. Biotechnol.* **2024**, *57*, 103106. [CrossRef]
56. Cavalheiro, C.V.; Picoloto, R.S.; Cichoski, A.J.; Wagner, R.; de Menezes, C.R.; Zepka, L.Q.; Da Croce, D.M.; Barin, J.S. Olive leaves offer more than phenolic compounds–Fatty acids and mineral composition of varieties from Southern Brazil. *Ind. Crops Prod.* **2015**, *71*, 122–127. [CrossRef]

57. Bahloul, N.; Kechaou, N.; Mihoubi, N.B. Comparative investigation of minerals, chlorophylls contents, fatty acid composition and thermal profiles of olive leaves (*Olea europeae* L.) as by-product. *Grasas Aceites* **2014**, *65*, e035. [CrossRef]
58. Alvarez, H.M.; Herrero, O.M.; Silva, R.A.; Hernández, M.A.; Lanfranconi, M.P.; Villalba, M.S. Insights into the metabolism of oleaginous *Rhodococcus* spp. *Appl. Environ. Microbiol.* **2019**, *85*, e00498-19. [CrossRef]
59. Herrero, O.M.; Moncalian, G.; Alvarez, H.M. Physiological and genetic differences amongst *Rhodococcus* species for using glycerol as a source for growth and triacylglycerol production. *Microbiology* **2016**, *162*, 384–397. [CrossRef]
60. Alvarez, H.M.; Mayer, F.; Fabritius, D.; Steinbüchel, A. Formation of intracytoplasmic lipid inclusions by *Rhodococcus opacus* strain PD630. *Arch. Microbiol.* **1996**, *165*, 377–386. [CrossRef]
61. Herrero, O.M.; Alvarez, H.M. Whey as a renewable source for lipid production by *Rhodococcus* strains: Physiology and genomics of lactose and galactose utilization. *Eur. J. Lipid Sci. Technol.* **2016**, *118*, 262–272. [CrossRef]
62. Van Wezel, G.P.; White, J.; Young, P.; Postma, P.W.; Bibb, M.J. Substrate induction and glucose repression of maltose utilization by *Streptomyces coelicolor* A3 (2) is controlled by malR, a member of the lacI–galR family of regulatory genes. *Mol. Microbiol.* **1997**, *23*, 537–549. [CrossRef]
63. Alvarez, H.M.; Kalscheuer, R.; Steinbüchel, A. Accumulation of storage lipids in species of *Rhodococcus* and *Nocardia* and effect of inhibitors and polyethylene glycol. *Lipid/Fett* **1997**, *99*, 239–246. [CrossRef]
64. Wältermann, M.; Luftmann, H.; Baumeister, D.; Kalscheuer, R.; Steinbüchel, A. *Rhodococcus opacus* strain PD630 as a new source of high-value single-cell oil? Isolation and characterization of triacylglycerols and other storage lipids. *Microbiology* **2000**, *146*, 1143–1149. [CrossRef] [PubMed]
65. Kohlmeier, M.G.; Oresnik, I.J. The transport of mannitol in *Sinorhizobium meliloti* is carried out by a broad-substrate polyol transporter SmoEFGK and is affected by the ability to transport and metabolize fructose. *Microbiology* **2023**, *169*, 001371. [CrossRef] [PubMed]
66. Sola-Carvajal, A.; García-García, M.I.; García-Carmona, F.; Sánchez-Ferrer, Á. Insights into the evolution of sorbitol metabolism: Phylogenetic analysis of SDR196C family. *BMC Evol. Biol.* **2012**, *12*, 147. [CrossRef] [PubMed]
67. Amara, S.; Seghezzi, N.; Otani, H.; Diaz-Salazar, C.; Liu, J.; Eltis, L.D. Characterization of key triacylglycerol biosynthesis processes in rhodococci. *Sci. Rep.* **2016**, *6*, 24985. [CrossRef]

Disclaimer/Publisher's Note: The statements, opinions and data contained in all publications are solely those of the individual author(s) and contributor(s) and not of MDPI and/or the editor(s). MDPI and/or the editor(s) disclaim responsibility for any injury to people or property resulting from any ideas, methods, instructions or products referred to in the content.